

Tessellated and stellated invisibility

André Diatta,¹ André Nicolet,² Sébastien Guenneau,¹ and Frédéric Zolla²

October 24, 2018

¹Department of Mathematical Sciences, Peach Street, Liverpool L69 3BX, UK

Email addresses: adiatta@liv.ac.uk; guenneau@liv.ac.uk

²*Institut Fresnel, UMR CNRS 6133, University of Aix-Marseille III, case 162, F13397 Marseille Cedex 20, France*

Email addresses: andre.nicolet@fresnel.fr; frederic.zolla@fresnel.fr;

Abstract

We derive the expression for the anisotropic heterogeneous matrices of permittivity and permeability associated with two-dimensional polygonal and star shaped cloaks. We numerically show using finite elements that the forward scattering worsens when we increase the number of sides in the latter cloaks, whereas it improves for the former ones. This antagonistic behavior is discussed using a rigorous asymptotic approach. We use a symmetry group theoretical approach to derive the cloaks design.

Ocis: (000.3860) *Mathematical methods in physics*; (260.2110) *Electromagnetic theory*; (160.3918) *Metamaterials*; (160.1190) *Anisotropic optical materials*

1 Introduction

Back in 2006, a team led by Pendry and Smith theorized and subsequently experimentally validated that a finite size object surrounded by a spherical coating consisting of a metamaterial might become invisible for electromagnetic waves [1, 2]. Many authors have since then dedicated a fast growing amount of work to the invisibility cloaking problem. However, there are alternative approaches, including inverse problems's methods [3] or plasmonic properties of negatively refracting index materials [4]. It is also possible to cloak arbitrarily shaped regions, and for cylindrical domains of arbitrary cross-section, one can generalize [1] to linear radial geometric transformations [5]

$$\begin{cases} r' &= R_1(\theta) + r(R_2(\theta) - R_1(\theta))/R_2(\theta), \quad 0 \leq r \leq R_2(\theta), \\ \theta' &= \theta, \quad 0 < \theta \leq 2\pi, \\ x'_3 &= x_3, \quad x_3 \in \mathbb{R}, \end{cases} \quad (1)$$

where r' , θ' and x'_3 are “radially contracted cylindrical coordinates” and (x_1, x_2, x_3) is the Cartesian basis. This transformation maps the arbitrary domain $D_{R_2(r,\theta)}$ onto

the coating $D_{R_2(r,\theta)} \setminus D_{R_1(r,\theta)}$ with $R_1(r,\theta) < R_2(r,\theta)$. In other words, if a source located in $\mathbb{R}^2 \setminus D_{R_2(r,\theta)}$ radiates in a vacuum, the electromagnetic field cannot reach the domain $D_{R_1(r,\theta)}$ and therefore this region is a shelter for any object. Moreover, the transformation maps the field within the domain $D_{R_2(r,\theta)}$ onto itself by the identity transformation. In this paper, we would like to investigate designs of polygonal and

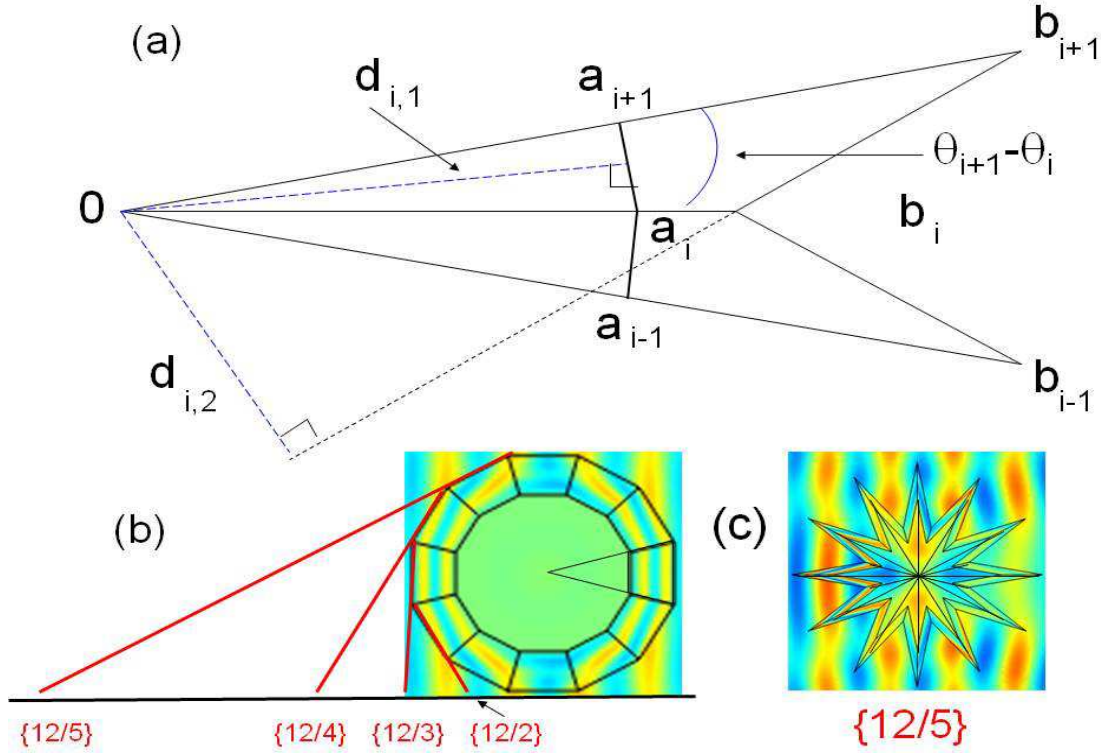


Figure 1: (a) Triangle of vertices $(0, 0)$, (b_i, θ_i) and (b_{i+1}, θ_{i+1}) used in the triangulation of a polygon (see (b)) or a polygram (see (c)) mapped under Eq. (1) onto the trapezoid of vertices (a_i, θ_i) , (b_i, θ_i) , (b_{i+1}, θ_{i+1}) and (a_{i+1}, θ_{i+1}) . The angles θ_i and the segments $d_{i,j}$ are as in Eq. (2); (b) Dodecagon and first step in its four tessellations $\{12/2\}$ - $\{12/5\}$; (c) Tessellation $\{12/5\}$ and representative samples of its triangulation.

star-shaped cloaks which we can triangulate, see Figs. 1, 2, 3. In this case, consider a given triangle, numbered i , of the triangulation of the region we want to cloak. We adapt Eqs. (1) to the specific geometry of triangles, to derive a geometric transform that maps the whole triangle of vertices $(0, 0)$, (b_i, θ_i) , (b_{i+1}, θ_{i+1}) onto a trapezoidal region of vertices (a_i, θ_i) , (a_{i+1}, θ_{i+1}) , (b_i, θ_i) , (b_{i+1}, θ_{i+1}) , see Fig. 1. This means that in Eqs. (1), the points $(R_1(\theta), \theta)$ and $(R_2(\theta), \theta)$ which now respectively lie in the line segments $[(a_i, \theta_i), (a_{i+1}, \theta_{i+1})]$ and $[(b_i, \theta_i), (b_{i+1}, \theta_{i+1})]$, are referred to as $(R_{i,1}(\theta), \theta)$ and $(R_{i,2}(\theta), \theta)$ where

$$\begin{cases} R_{i,j} = d_{i,j} / \cos(\theta - \theta_0), & \theta_i \leq \theta \leq \theta_{i+1}, \quad j = 1, 2 \\ d_{i,j} = c_{i,j} c_{i+1,j} \sin(\theta_{i+1} - \theta_i) / \sqrt{c_{i,j}^2 + c_{i+1,j}^2 - 2c_{i,j} c_{i+1,j} \cos(\theta_{i+1} - \theta_i)}, & j = 1, 2 \\ \theta_0 = \theta_i + \arccos(d_{i,j} / c_{i,j}) = \theta_{i+1} + \arccos(d_{i,j} / c_{i+1,j}) \\ c_{i,1} = a_i, \quad c_{i,2} = b_i \end{cases}$$

In the sequel, we make use of symmetries to further simplify the implementation of such cloaks. More precisely, we work in a reference triangle and construct the overall cloak via compound reflection symmetries and rotations from this reference region.

2 Change of coordinates and pullbacks from optical to physical space

The basic principle of our approach is to transform a geometrical domain into another one and to search how the Maxwell equations to be solved have to be changed. As we start with a given set of equations on a given domain, it seems at first sight that we have to map this domain on a new one. Nevertheless, it is the opposite that has to be done. On the original domain, say Ω , the equations are described in a particular coordinate system x_i (taken here by default to be Cartesian coordinates). We want to establish a one-to-one correspondence with a new domain Ω' where we use a general (possibly non-orthogonal) coordinate system y_i .

$$\begin{array}{ccc}
 \text{domain } \Omega \text{ with} & \longleftarrow & \text{domain } \Omega' \text{ with} \\
 \text{coordinates } x_i & x_i(y_j) & \text{coordinates } y_i \\
 \\
 \text{differential } dx_i & \longrightarrow & \text{differential } \sum_j \frac{\partial x_i(y_j)}{\partial y_j} dy_j \\
 \text{pullback} & &
 \end{array} \tag{2}$$

More precisely, consider a map from a coordinate system $\{y_1, y_2, y_3\}$ to the initial one $\{x_1, x_2, x_3\}$ given by the transformation $x_1(y_1, y_2, y_3)$, $x_2(y_1, y_2, y_3)$ and $x_3(y_1, y_2, y_3)$. Here, we must point out that, we are mapping the transformed domain and coordinate system onto the initial one with Cartesian coordinates. This change of coordinates is characterized by the transformation of the differentials through $d\mathbf{x} = \mathbf{J}_{xy} d\mathbf{y}$ where

$$\mathbf{J}_{xy} = \frac{\partial(x_1, x_2, x_3)}{\partial(y_1, y_2, y_3)}, \quad d\mathbf{x} = (dx_1, dx_2, dx_3)^T \text{ and } d\mathbf{y} = (dy_1, dy_2, dy_3)^T. \tag{3}$$

In the sequel we will also need a compound transformation. Let us consider three coordinate systems $\{y_1, y_2, y_3\}$, $\{z_1, z_2, z_3\}$, and $\{x_1, x_2, x_3\}$ (possibly on different regions of spaces). The two successive changes of coordinates are given by the Jacobian matrices \mathbf{J}_{xz} and \mathbf{J}_{zy} . This rule naturally applies for an arbitrary number of coordinate systems and we call the resulting Jacobian matrix $\mathbf{J} = \mathbf{J}_{xz} \mathbf{J}_{zy}$. In electromagnetism, changes of coordinates amount to replacing the different materials (often homogeneous and isotropic, which corresponds to the case of scalar piecewise constant permittivity ε and permeability μ) by equivalent inhomogeneous anisotropic materials described by a transformation matrix \mathbf{T} (metric tensor) [6, 7, 8, 9] so that the new permittivities and permeabilities read

$$\underline{\underline{\varepsilon}}' = \varepsilon \mathbf{T}^{-1}, \quad \text{and} \quad \underline{\underline{\mu}}' = \mu \mathbf{T}^{-1} \text{ where } \mathbf{T} = \mathbf{J}^T \mathbf{J} / \det(\mathbf{J}). \tag{4}$$

3 Transformation optics and the geometry of irregular polygons

3.1 Material properties of the regions

From Eqs. (1), (2) and (4), we derive the transformation matrix associated with a reference trapezoidal region (see Fig. 1) used to generate, via reflections symmetry and rotations, two-dimensional polygonal and star-shaped cloaks:

$$\mathbf{T}^{-1} = \begin{pmatrix} \frac{e_{12}^2 + f_r^2}{e_{11} f_r r'} & -\frac{e_{12}}{f_r} & 0 \\ -\frac{e_{12}}{f_r} & \frac{e_{11} r'}{f_r} & 0 \\ 0 & 0 & \frac{e_{11} f_r}{r'} \end{pmatrix}, \quad (5)$$

where

$$e_{11}(\theta') = R_2(\theta') / (R_2(\theta') - R_1(\theta')) \quad (6)$$

and

$$e_{12}(r', \theta') = \frac{(r' - R_2(\theta')) R_2(\theta') \frac{dR_1(\theta')}{d\theta'} - (r' - R_1(\theta')) R_1(\theta') \frac{dR_2(\theta')}{d\theta'}}{(R_2(\theta') - R_1(\theta'))^2} \quad (7)$$

for

$$R_1(\theta') \leq r' \leq R_2(\theta'), \quad (8)$$

with

$$f_r(r', \theta') = (r' - R_1(\theta')) \frac{R_2(\theta')}{R_2(\theta') - R_1(\theta')} \quad (9)$$

(the expression for e_{12} corrects that in [5]). Elsewhere, \mathbf{T}^{-1} reduces to the identity matrix ($e_{11} = 1$, $e_{12} = 0$ and $f_r = r'$ for $r' > R_2(\theta')$). However, Eqs. (4) and (5) can just be applied to derive the (anisotropic heterogeneous) permittivity $\underline{\underline{\epsilon}}'$ and permeability $\underline{\underline{\mu}}'$ in the reference triangle. An elegant way to deduce optical properties of other regions of the triangulation is to use linear groups of symmetry in the plane, as now explained.

3.2 Symmetries and transformation groups in cloaks' construction

Here, we use Euclidean groups, namely reflections symmetry and rotations in the plane, as a tool to design very general polygonal and star-shaped cloaks. We choose our reference triangle (labeled as triangle number 1, or just referred to as first triangle) to be in the first quadrant with one of its sides belonging to the x_1 -axis. In the regular polygons case, the triangle number i of the triangulation, is simply obtained from this first one, via the rotation with angle $(i - 1)\frac{\pi}{n}$. In the irregular case (star-shaped), due

to geometric chirality properties (irregular triangles are not identical to their mirror images), triangles of odd numbers cannot be obtained by rotations from the original one. More precisely, the neighboring triangles are obtained, from the first one, as mirror images with respect to the shared side (more precisely, a mirror image with respect to the plane perpendicular to the triangle and containing the shared side). Hence, any triangle of even number i , is obtained by applying to the first triangle the linear map

$$(x_1, x_2) \mapsto (x_1 \cos(\frac{\pi}{n}i) + x_2 \sin(\frac{\pi}{n}i), x_1 \sin(\frac{\pi}{n}i) - x_2 \cos(\frac{\pi}{n}i)) \quad (10)$$

which is the composition of the reflection $(x_1, x_2) \mapsto (x_1, -x_2)$ with respect to x_1 -axis, followed by the rotation with angle $\frac{\pi}{n}i$. Whereas, every triangle of odd number i , is obtained by rotating the first triangle with angle $(i-1)\frac{\pi}{n}$. In short, optical properties of all regions within the triangulation are deduced from the reference trapezoidal region using compositions of rotations and reflections. This algorithm is particularly well-suited for all polygonal or star shaped regions displaying n -fold symmetries.

3.3 Tessellation and stellation

We are interested in the antagonistic behaviour of polygonal and star shaped cloaks. There is a natural correspondence between these two types of cloaks, and this can be seen as follows.

Consider a regular star polygon which is represented by its Schläfli symbol $\{n/m\}$, where n is the number of vertices, and m is the step used in sequencing the edges around it. For example, take a dodecagram $\{12/5\}$ as in Fig. 1 which has twelve vertices, see Fig. 3(c). One can draw a straight line joining each of its vertices to another one, which is five vertices apart. Or equivalently, choose a vertex, say, on the horizontal axis and project the other vertices onto that axis as depicted in Fig. 1(b). For a given dodecagon with Schläfli symbol $\{12\}$, there are four segments obtained by projection which generate four distinct stellations $\{12/2\}$ - $\{12/5\}$. Note that a regular polygon with n sides has $(n-4)/2$ stellations if n is even, and $(n-3)/2$ stellations, if n is odd. We display in Fig. 2 and 3 a gallery of cloaks together with their Schläfli symbol. We note that the higher the Schläfli symbol of the polygons, the smoother the wave patterns (the less scattering).

On the contrary, the scattering worsens for their corresponding stellations. This is not surprising since it is fairly intuitive that a cloak with many sharp angles will tend to display more singularities in the entries of the transformation matrix describing the electromagnetic material properties. However, we now give an asymptotic argument supporting this numerical observation.

3.4 Asymptotic behaviour of the T^{-1} matrix

The tessellation of regular polygons involves n regular triangles. We can chose

$$a_i = a_{i+1} =: R_1, \quad b_i = b_{i+1} =: R_2, \quad \theta_{i+1} - \theta_i = \frac{\pi}{n} \quad \text{and} \quad \theta = s\frac{\pi}{n}, \quad 0 \leq s \leq 1. \quad (11)$$

The coefficients of \mathbf{T}^{-1} now read

$$\begin{aligned}
T_{11}^{-1} &= \frac{r' - R_1}{r'} + O\left(\frac{1}{n^2}\right), \\
T_{22}^{-1} &= \frac{r'}{r' - R_1} + O\left(\frac{1}{n^2}\right), \\
T_{33}^{-1} &= \left(\frac{R_2}{R_2 - R_1}\right)^2 \frac{r' - R_1}{r'} + O\left(\frac{1}{n^2}\right), \\
T_{12}^{-1} &= T_{21}^{-1} = -\frac{\pi R_1 (r' + 2s(r' - R_1))}{2r'(r' - R_1)} \frac{1}{n} + O\left(\frac{1}{n^3}\right),
\end{aligned} \tag{12}$$

and $T_{ij}^{-1} = 0$, otherwise. So as n grows, \mathbf{T}^{-1} tends to

$$\mathbf{T}_\infty^{-1} = \text{Diag}\left(\frac{r' - R_1}{r'}, \frac{r'}{r' - R_1}, \left(\frac{R_2}{R_2 - R_1}\right)^2 \frac{r' - R_1}{r'}\right). \tag{13}$$

This is the expression of the transformation matrix for a circular cloak, see also [10] for a particular case. Now assume $a_{i+1} \neq a_i$, or $b_{i+1} \neq b_i$, which is expected to hold in star shaped case, the Taylor expansion shows that, at least one T_{ij}^{-1} tends to infinity or $\det(\mathbf{T}^{-1})$ tends to zero, as n increases. For example,

$$T_{11}^{-1} = \frac{-(a_{i+1} - a_i)^2 a_i^2 a_{i+1}^2}{(r' s(a_{i+1} - a_i) + a_{i+1}(r' - a_i))(a_{i+1} + s(a_{i+1} - a_i))^3 \pi^2 r'} n^2 + O(1), \tag{14}$$

if $a_{i+1} > a_i$ and $b_{i+1} > b_i$. This explains the origin of the singularities in the material parameters of stellated cloaks.

4 Finite elements computations

Let us now compute the total electromagnetic field for a plane wave incident upon a cylindrical cloak. In p polarization, if \mathbf{e}_3 is a unit vector oriented along the axis of the cylinder, the longitudinal electric field $\mathbf{E}_l = E_3(x_1, x_2)\mathbf{e}_3$ is solution of:

$$\nabla \times \left(\underline{\underline{\mu}}'^{-1} \nabla \times \mathbf{E}_l \right) - k^2 \underline{\underline{\varepsilon}}' \mathbf{E}_l = \mathbf{0} \tag{15}$$

where $k = \omega \sqrt{\mu_0 \varepsilon_0} = \omega/c$ is the wavenumber, c being the speed of light in vacuum, and $\underline{\underline{\varepsilon}}'$ and $\underline{\underline{\mu}}'$ are defined by Eqs. (4) and (5). Also, $\mathbf{E}_l = \mathbf{E}_i + \mathbf{E}_d$, where $\mathbf{E}_i = e^{ikx_1} \mathbf{e}_3$ is the incident field and \mathbf{E}_d is the diffracted field which satisfies the usual outgoing wave condition (to ensure existence and uniqueness of the solution). We have implemented the weak form of this scattering problem in the finite element package COMSOL (with Perfectly Matched Layers modelling the unbounded domain). We consider a plane wave incident from the left at wavelength $\lambda = 0.35$ (*all lengths are given in arbitrary units, μm for instance*). We note that when we increase the number of sides of a polygonal cloak, the scattering becomes less apparent in Fig. 2, which is in agreement with the fact that the transformation matrix \mathbf{T}^{-1} tends to that of a circular cloak, see formula (13). On the contrary, both forward and backward scattering worsen when we increase

the number of sides of corresponding stellated (star-shaped) cloaks, see Fig. 3, and we have identified the origin of this singular behaviour in the previous section. Note that we kept the frequency constant as well as the mesh (with around 60.000 elements), so as to exemplify that any attempt to manufacture a star-shaped cloak with many sides would be fairly challenging: when we refine the mesh, the scattering indeed reduces suggesting severer constraints on the corresponding metamaterial. Interestingly, the field can be confined when the frequency of the plane wave excites some resonance of the star-shaped cavity inside the cloak, see Fig. 3 (f).

5 Conclusion

Analysis of polygonal invisibility cloaks is of current interest [10, 11, 12]. In this paper, we made use of a symmetry group action to construct such cloaks, and we have numerically shown that, for a given frequency, n -sided polygonal cloaks behave in a way similar to circular cloaks when n increases whereas their stellated counterparts become more and more singular. An asymptotic algorithm supports these observations. A natural question to ask is whether it is possible to design such cloaks using a homogenization approach. Our analysis suggests that the answer should be positive for the former type of cloaks (as their boundary smoothens for large n and as it has been shown that structured circular cloaks can be homogenized [13]). We conjecture that the answer should be negative for the latter cloaks: it is well-known that homogenization theory fails in so-called bad domains that display boundaries with sharp corners (for which star-shaped invisibility cloaks is an electromagnetic paradigm).

Acknowledgments

A. Diatta and S. Guenneau acknowledge funding from EPSRC grant EP/F027125/1.

References

- [1] J.B. Pendry, D. Shurig, D.R. Smith, “Controlling electromagnetic fields,” *Science* **312**, 1780-1782 (2006).
- [2] D. Schurig, J.J. Mock, B.J. Justice, S.A. Cummer, J.B. Pendry, A.F. Starr, D.R. Smith, “Metamaterial electromagnetic cloak at microwave frequencies,” *Science* **314**, 977-980 (2006).
- [3] A. Greenleaf, M. Lassas and G. Uhlmann, “On nonuniqueness for Calderons inverse problem,” *Math. Res. Lett.* **10**, 685-693 (2003).
- [4] R.C. McPhedran, N.A. Nicorovici, G.W. Milton, “Optical and dielectric properties of partially resonant composites”, *Phys. Rev. B* **49**, 8479-8482 (1994).
- [5] Nicolet A, Zolla F, Guenneau S, ”Electromagnetic analysis of cylindrical cloaks of an arbitrary cross section.” *Opt. Lett.* **33**, 1584-1586 (2008).

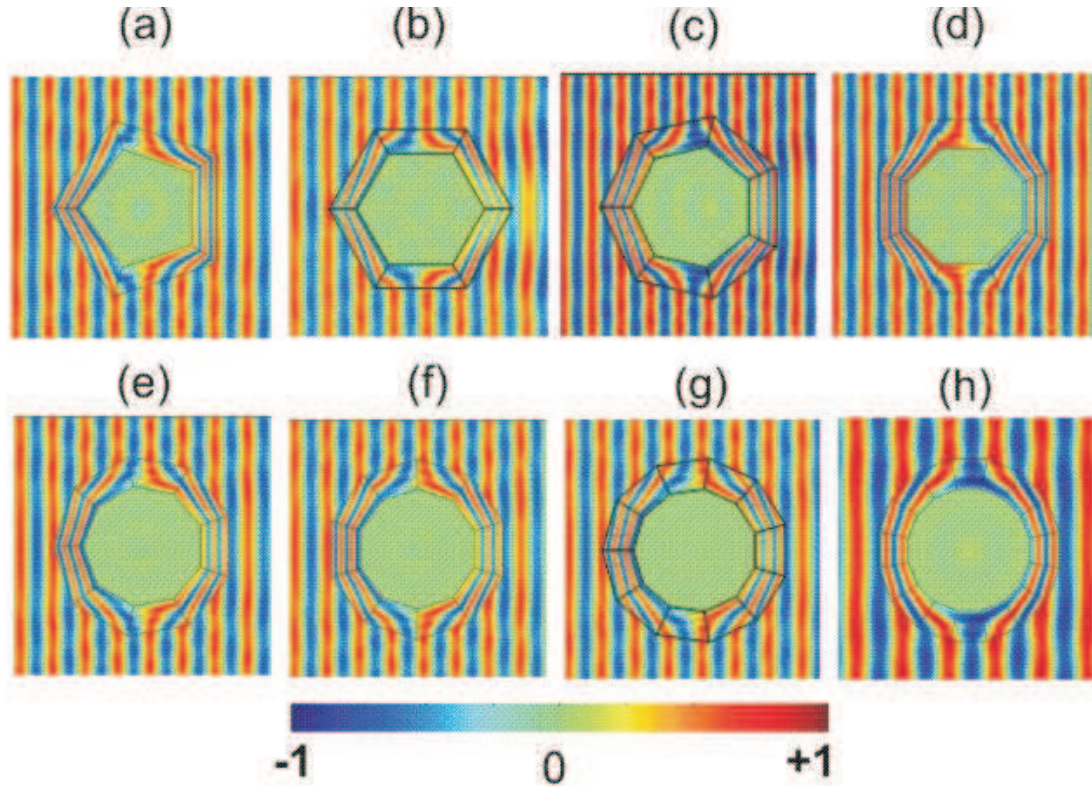


Figure 2: Real part of the longitudinal component E_3 of the electric field scattered by a (a) pentagon {5}, (b) hexagon {6}, (c) heptagon {7}, (d) octagon {8}, (e) nonagon {9}, (f) decagon {10}, (g) hendecagon {11} (h) hexadecagon {16} polygonal cloaks. Both forward and backward scattering for a plane wave propagating from the left are nearly vanishing.

- [6] A.J. Ward and J.B. Pendry, "Refraction and geometry in Maxwell's equations," *J. Mod. Opt.* **43**, 773-793 (1996).
- [7] A. Nicolet, J.F. Remacle, B. Meys, A. Genon, W. Legros, "Transformation methods in computational electromagnetism," *J. Appl. Phys.* **75**, 6036-6038 (1994).
- [8] F. Zolla, S. Guenneau, A. Nicolet and J.B. Pendry, "Electromagnetic analysis of cylindrical invisibility cloaks and the mirage effect", *Opt. Lett.* **32**, 1069-1071 (2007).
- [9] U. Leonhardt and T. G. Philbin, "General relativity in electrical engineering," *New J. Phys.* **8**, 247 (2006).
- [10] P.H. Tichit, B. Kante and A. de Lustrac, "Design of polygonal and elliptical cloaks", *Proceedings of Nato ARW and META08, Marrakesh-Morocco, 7-10 May (2008)*, 120-125.
- [11] J. Zhang, Y. Luo, H. Chen, and B. Wu, "Cloak of arbitrary shape," *J. Opt. Soc. Am. B* **25**, 1776-1779 (2008)

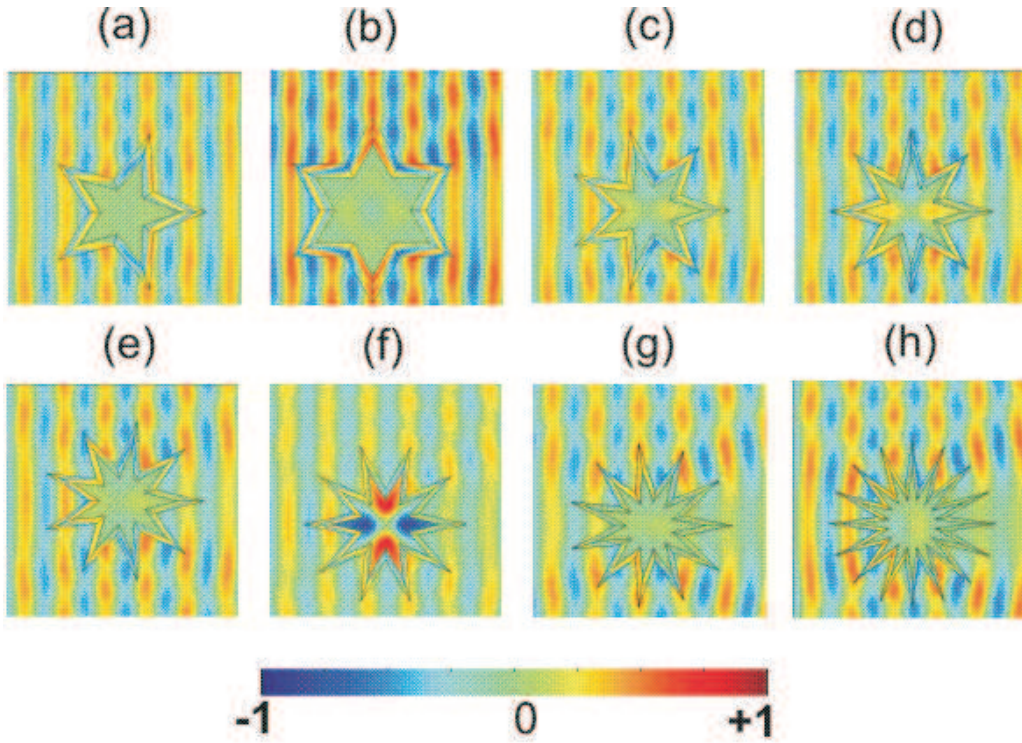


Figure 3: Real part of the longitudinal component E_3 of the electric field scattered by a (a) pentagram $\{5, 2\}$, (b) hexagram $\{6, 2\}$, (c) heptagram $\{7/3\}$, (d) octagram $\{8/3\}$, (e) nonagram $\{9/4\}$, (f) decagram $\{10/4\}$, (g) hendecagram $\{11/5\}$ (h) hexadecagram $\{16/7\}$ star-shaped cloaks. Unlike for computations reported in Figure 2, scattering worsens from panels (a) to (h), and most specifically forward scattering.

- [12] Chao Li and Fang Li, "Two-dimensional electromagnetic cloaks with arbitrary geometries," *Opt. Express* **16**, 13414-13420 (2008)
- [13] M. Farhat, S. Guenneau, A.B. Movchan and S. Enoch, "Achieving invisibility over a finite range of frequencies," *Opt. Express* **16**, 5656-5661 (2008)